Journal of Engineering Science and Technology
Vol. 13, No. 8 (2018) 2369 - 2378

PLASMA NITRIDING TIME ON THE HARDNESS AND CRYSTAL STRUCTURE/PHASE OF SUS403 AND SCS6 MARTENSITIC STAINLESS STEELS: AN ANALYTICAL STUDY

FARID TRIAWAN[1,*], ASEP BAYU DANI NANDIYANTO[2], ADE GAFAR ABDULLAH[3], MUHAMMAD AZIZ[4]

[1]Department of Mechanical Engineering, Sampoerna University,
Jl. Raya Pasar Minggu, Kav 16, Jakarta, Indonesia
[2]Departemen Kimia, Universitas Pendidikan Indonesia,
Jl. Dr. Setiabudi no 229, Bandung 40154, Indonesia
[3]Departemen Pendidikan Teknik Elektro, Universitas Pendidikan Indonesia,
Jl. Dr. Setiabudi no 229, Bandung 40154, Indonesia
[4]Institute of Innovative Research, Tokyo Institute of Technology,
2-12-1 Ookayama, Meguro-ku, Tokyo 152-8552 Japan
*Corresponding author: farid.triawan@sampoernauniversity.ac.id

Abstract

The purpose of this study is to analyze the effect of plasma nitriding time on the physicochemical properties and mechanical hardness of commercially available martensitic stainless steels, SUS403 (JIS G4304) and SCS6 (JIS G5121). Both steels were chosen as the model materials because of their general applications, such as for pressure vessel, valve, turbine, pump, and conveyor belt in petroleum industry, in which high strength and good corrosion resistant materials are demanded. The nitriding processes were carried out by plasma process at fixed temperature of 450°C with varied processing times of 20, 30, and 40 hours. The results show that the addition of nitrogen has a significant role in modifying the microstructure, phase balance, and hardness of both steels. Varying the processing time has a direct impact to the penetration depth of nitrogen into the material. Interestingly, despite similar martensitic properties, we found that the nitrided layer on SUS403 and SCS6 specimens exhibits different iron nitride layer characteristics, i.e., crystal structure/phase and hardness profile. It was revealed that the processing time of 20 hours is suitable to form an Fe_4N compound layer. Longer than this period is just increasing the iron-nitride layer thickness. In addition, the present study also discussed the formation process of iron nitride compound-layer during plasma nitriding process.

Keywords: Crystal structure, Hardness, Iron nitride, Martensitic stainless steel, Plasma nitriding.

1. Introduction

Iron nitride materials have given tremendously attentions for researchers due to their excellent performance compared to iron and iron oxide, such as magnetic properties [1, 2], corrosion resistance, catalytic performance [3], and mechanical strength [4]. The properties of iron nitride depend on the nitrogen component in the material [5].

To produce iron nitride, several technologies have been commercialized [6]:

(i) Gas nitriding. This process is carried out usually at temperatures of 550–580°C in a box furnace or fluidized bed in an atmosphere filled with partially dissociated ammonia. The major benefit from this process is that it can be done in a condition of the near-ideal temperature uniformity through the entire gas-particle volume and fast heating rate. The processing condition (i.e., time, temperature, and gas dissociation rate) can be controlled easily to get a product with specific properties.

(ii) Liquid salt nitriding. This process is conducted using the fused salt bath containing either cyanides or cyanates. A typical commercial bath that is typically used is a mixture of 60–70% of sodium salts (96.5% of NaCN, 2.5% of Na_2CO_3, and 0.5% of NaCNO) and 30–40% of potassium salts (96% of KCN, 0.6% of K_2CO_3, 0.75% of KCNO, and 0.5% of KCl). The major benefit is its simple and rapid processing cycle (due to intense heating and high reactivity of the medium).

(iii) Plasma nitriding. This process is conducted using a glow discharge phenomenon to introduce nitrogen to the surface of a metal via diffusion of nitrogen element. The major benefits include the relatively low temperature, short saturation time, and simple mechanical masking, as well as surface-activation sputtering.

(iv) Laser nitriding. This process uses a direct laser irradiation to the specimen that is placed in a reactive gas environment. The reactive gas, containing nitrogen, is fed through a nozzle into the melt pool. The process is feasible to be applied in industry; however, the nitriding process is limited to the laser irradiation area only, making it difficult to be applied into large area of metal.

(v) Beam ion implantation. This process used an ion beam to incorporate nitrogen into a material surface. Although this method is prospective for industry, this technique requires exploration of elevated temperatures, in which the temperature must be done at higher than 600°C.

Among the above techniques, plasma nitriding is usually considered as the simplest technique to produce iron nitride structure on a steel material. This is because the thickness of nitrided layer on the entire specimen body can be controlled easily by changing the process parameters, such as nitrogen gas flow and composition, processing time, and temperature, as well as pressure. Indeed, plasma nitriding technique has been widely utilized to improve the wear resistance of steel component for enhancing its service life [7, 8]. Moreover, the hardened surface could avoid damage and failure of machine components due to external loads [9-11]. Thus, understanding the optimum process parameters to get excellent product can give advantages and information for further development in the production of nitrided materials.

Many papers have discussed the strategies on the production of iron nitride [1-5, 12-18]. Some also reported the use of commercially available martensitic

stainless steels, such as AISI 410 [19], AISI 420 [7, 20], and AISI 440C [21]. However, to the best of our knowledge, report on the effect of plasma nitriding time on the physicochemical properties and mechanical hardness of SUS403 (JIS G4304) and SCS6 (JIS G5121) is very limited.

The purpose of this study was to analyze the effect of nitriding time by plasma synthesis process to commercially available martensitic stainless steels SUS403 (JIS G4304) and SCS6 (JIS G5121). Both steels were chosen because of their wide range of applications, such as for pressure vessel, valve, turbine, pump, and conveyor belt in petroleum industry, in which high strength and good corrosion resistant materials are demanded. Plasma nitriding technique was selected since the process offers the ability in improving the surface hardness while neither sacrificing the corrosion resistance nor changing the major volume of the parent material.

The present work extends the experimental results reported by Liem et al. [8] in order to perform an analytical study on the formed iron-nitrided layer. We showed that the addition of nitrogen has a significant role on the microstructure, phase balance, and surface hardness of the both steels. Interestingly, we found that both steels showed different iron nitride characteristics despite their similar martensitic stainless steel properties. The present study was also completed with a discussion on iron-nitride formation mechanism during the nitriding process.

2. Experimental Method

The present study used two types of martensitic stainless steels: SUS403 (JIS G4303) and SCS6 (JIS G5121). According to the Japanese Industrial Standard (JIS), SUS403 is classified as a hot-rolled stainless steel and SCS6 is as a cast stainless steel, both possess a good corrosion resistance. All samples were manufactured by a wire-cutting machine with a specific dimension of length, width, and thickness of 15, 10, and 5 mm, respectively. Detailed elemental composition of the two types of stainless steel is described in Table 1.

Table 1. Elemental composition of SUS403 and SCS6 [8].

Element	Elemental composition (wt%)	
	SUS403	SCS6
Carbon	0.13	0.03
Silica	0.44	0.39
Manganese	0.44	0.36
Phosphor	0.027	0.019
Sulfur	0.024	0.009
Nickel	0.20	3.81
Chromium	11.77	13.10
Molybdenum		0.60

The samples of both steels were then put into a plasma nitriding apparatus, which was conducted at a temperature of 450°C and a pressure of 800 $\pm$ 200 Pa. To support the nitriding process, the plasma process was introduced with a reactant gas, consisting of 25% of nitrogen (N_2) and 75% of hydrogen (H_2). The processing time was varied for 20, 30, and 40 hours.

To characterize the successfulness of nitriding process, the nitrided samples were analyzed using an X-Ray Diffraction (XRD; Multiflex, Rigaku, Japan). The hardness profile of the nitrided samples were measured by micro Vickers hardness

test (JIS 2244) on the cross sectional area over a distance of 500 μm from the sample surface.

3. Results and Discussion

3.1. XRD analysis result

Figure 1 shows the XRD analysis results for the SUS403 sample before and after the nitridation. The paneled image is the photograph of the sliced sample after the nitridation at processing time of 40 hours. As seen in the figure, nitrided layer is formed after nitriding process (dark area between brighter area and dashed (surface) line). The thickness of the nitrided layer is more than 100 μm. Then, the nitrided layer was taken and analyzed using XRD.

The nitriding time was varied at 20, 30, and 40 hours. As standard evaluations, the XRD analysis was compared to the Joint Committee of the Powder Diffraction System (JCPDS) no 06-0696, 72-2126, 72-2125, and 86-0231, corresponding to Fe, Fe_2N, Fe_3N, and Fe_4N, respectively. The result shows that the initial SUS403 contains Fe pattern. Although SUS403 contains other components (such as nickel, chrome, etc.), as shown in Table 1, the peaks of these components were not detected. The composition of these components is too little to be identified.

After the nitriding process, several peaks were detected. For 20 hours of the nitriding process, there are additional peaks to the initial Fe peaks, i.e., Fe_2N, Fe_3N, and Fe_4N. After nitridation of 30 hours, Fe_3N peaks disappeared, whereas Fe_4N dominated the structure. Finally, after conducting nitridation for 40 h, XRD pattern contained mostly Fe_4N and some Fe_2N.

Figure 2 shows the XRD analysis results for the SCS6 sample before and after nitriding process at 20, 30, and 40 h, compared to the JCPDS no 06-0696, 72-2126, 72-2125, and 86-0231 for Fe, Fe_2N, Fe_3N, and Fe_4N, respectively. The paneled image is the photograph of the sliced sample after the nitriding process. Different from the nitrided SUS403 shown in Fig. 1, the nitrided layer in SCS6 is relatively thinner (about 75 μm).

As shown in Figs. 1 and 2, we found that no FeN was detected in all samples. This confirmed that the process can not make more penetration of nitrogen element into the Fe atomic structures. Also, different from our previous studies [2, 14, 17, 18], no $Fe_{16}N_2$ pattern was detected in the samples, in which this is because the present process is not compatible to further change the crystal structure from Fe to form $Fe_{16}N_2$.

Based on the above process, the present process is effective to produce an iron nitride layer (see Figs. 1 and 2) on both steels. The nitriding time of 20 hours at 450°C was found to be effective in creating the Fe_4N compound. Longer than this period was just increasing the iron-nitride layer thickness.

The XRD analysis results of the initial SCS6 show the detection of the Fe pattern only, which is similar to the SUS403 sample in Fig. 1. After the nitriding process, several peaks were identified. The nitriding process for 20 hours results in additional Fe_2N, Fe_3N, and Fe_4N peaks. Then, after conducting nitridation for 30 and 40 hours, Fe_3N peaks disappeared, whereas Fe_4N dominated the structure.

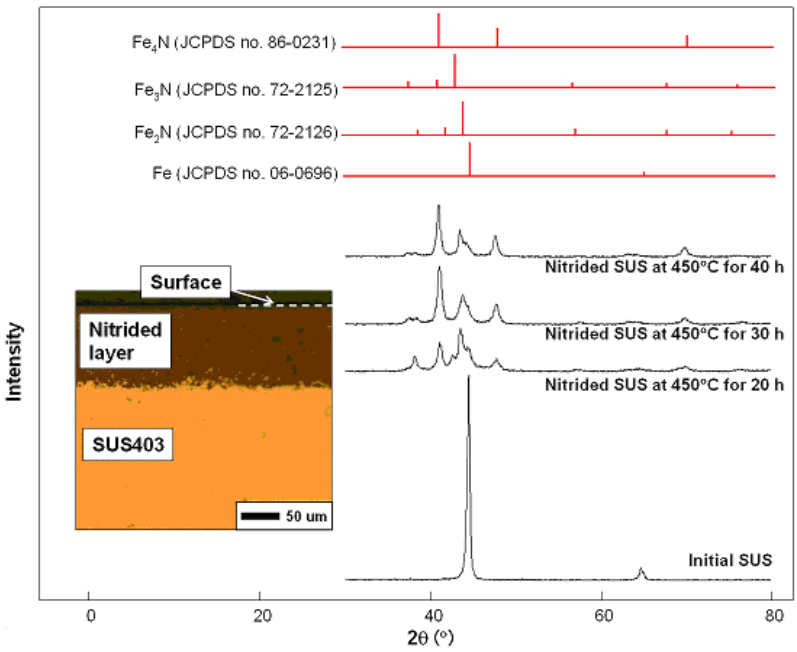

Fig. 1. The XRD analysis results of SUS403 nitrided with various processing times. The paneled image is the photograph of the sliced nitrided sample processed for 40 hours.

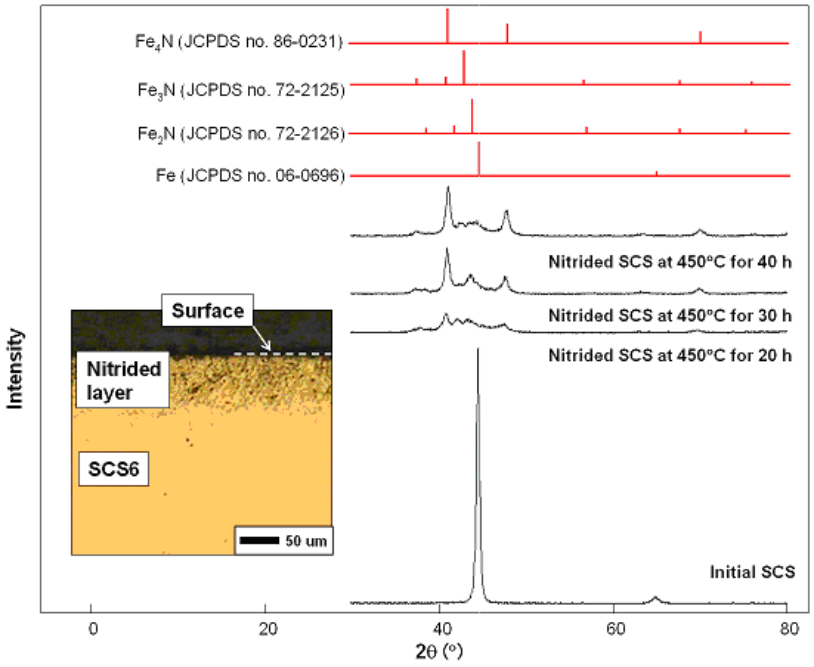

Fig. 2. The XRD analysis results of SCS6 nitrided with various processing times. The paneled image is the photograph of the sliced nitrided sample for 40 hours processing time.

A proposal on the formation mechanism of nitrided layer in a martensitic stainless steel is presented in Fig. 3. In simplification of the process, viz. Fig. 3(a), the existence of H_2 gas can hydrogenise the protection layer (as chromium does in forming oxide chromium (CrO_2)) on the surface of stainless steel [6], while the presence of N_2 gas is effective as the nitrogen source [1]. The hydrogenation removes the oxide component to form their originated metal component [14]. At the same time with the hydrogenation, N_2 gas is converted into radical nitrogen [16]. Since the protective layer has been removed, radical nitrogen can move from the plasma to the material sub-surface. Then, this radical nitrogen penetrates into the atomic iron interstitial. Consequently, the atomic structure is changed from body centered tetragonal (for martensitic steel material) to the Fe_4N structure, refer to Fig. 3(b). The penetration occurs on the entire surface, forming Fe_4N layer. The nitrogen penetration process depends on the diffusion time of the material. Thus, increasing processing time results in the deeper formation of iron nitride layer.

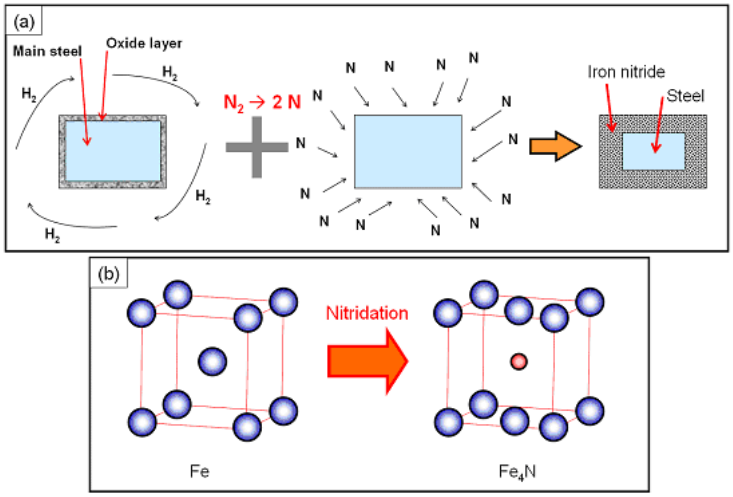

Fig. 3. Proposal mechanism for the formation of Fe_4N material structure. Figure (a) is the proposal mechanism in the physical appearance, whereas Fig. (b) is that in the atomic structure.

In addition to the formation of layer, there is a chemical reaction during the penetration of nitrogen element into Fe atomic structure. Nitrogen moves step by step to the Fe atomic structure to form Fe_2N, Fe_3N, and Fe_4N. This is confirmed by the existence of this iron nitride XRD patterns after 20 hours of reaction (Figs. 1 and 2). Further additional processing time allows the nitrogen radical to go further into deeper position of the Fe atomic structure. The conversion of Fe_2N and Fe_3N into Fe_4N structure was also found. Among these three types of iron nitrides, Fe_3N is the weakest. Fe_3N is easily changed into Fe_4N. That is the main fundamental reason why the Fe_3N is not detected after more than 30 hours of nitridation.

3.2. Micro Vickers hardness test result

The results of the Vickers hardness measurements on both steels along the cross-sectional path from the surface are given in Fig. 4 [8]. In the figure, the hardness profile of SUS403, Fig. 4(a) and SCS6, Fig. 4(b) samples under different

nitridation times are plotted and compared. The results exhibit that the hardness values of nitrided samples are higher than that of initial samples (prior to the nitriding process). Hardness values of the initial SUS403 and SCS6 are 170 and 285 HV, respectively (horizontal dashed line in Figs. 4(a) and (b). According to the hardness profile, nitriding process can improve the hardness to more than 4 times of their initial condition. Additional nitridation has a direct impact to the improvement of hardness, in which this is in a good agreement with previous studies [7, 19, 20, 22, 23].

The successful hardening material in changing Fe into Fe_4N is due to the change in the atomic structure from Fe to Fe_4N, confirmed by XRD analysis results in Figs. 1 and 2. The atomic structure in iron nitride material is more pack that that in the Fe atomic structure only, Fig. 3(b).

Measurement on both steels at the surface (0 μm in distance) gives almost equal hardness value of 1200 HV. This result agreed well with the previous reports that used different martensitic stainless steels and processed at different conditions [7, 19, 20]. Since all variations of processing time gave the same value of hardness at the surface, it demonstrated that plasma nitriding within 20 hours is sufficient to produce a SUS403 or SCS6 martensitic stainless steel with a surface hardness of around 1200 HV. This also confirms that differences in the use of SUS403 and SCS6 samples seem to have less significant impact to the difficult formation of Fe_4N compound layer. This is quite interesting since there is a considerable difference in the elemental composition in both types of stainless steels as shown in Table 1.

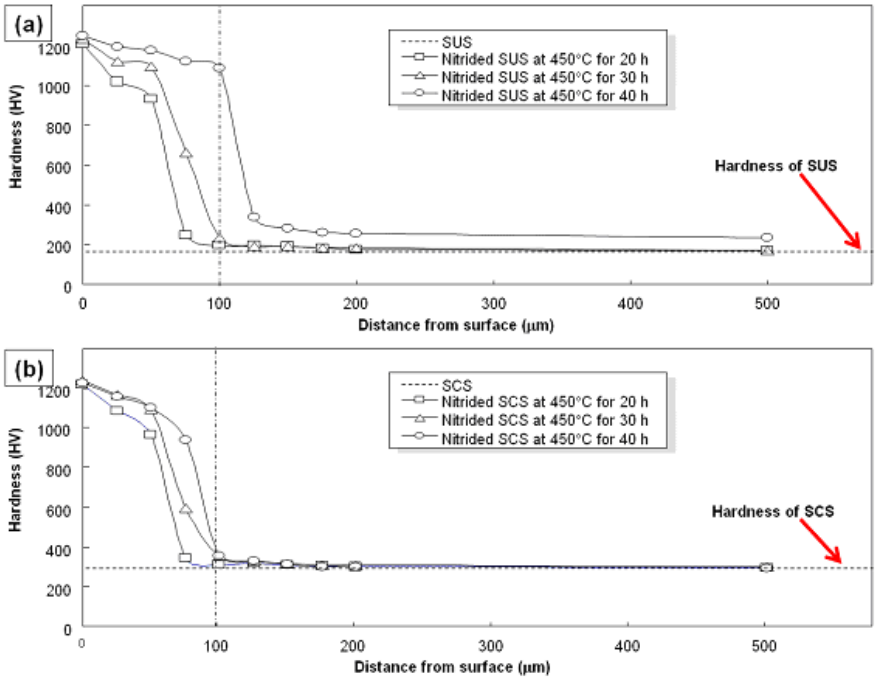

Fig. 4. Micro Vickers hardness test results of SUS403 (a) and SCS6 (b) nitrided under various processing times.

The deeper distance from the surface leads to the decreasing hardness values. The decrease in the hardness is due to the different compositions of iron nitride structure. The more amounts of Fe_4N structure makes the harder material can be obtained. Indeed, the deeper distance will be in line with the less number of Fe_4N. In addition, although Fe_2N and Fe_3N may give an impact to the improvement of hardness, their influences are not as big as Fe_4N does.

Comparing the SUS403 and the SCS6 samples, the SUS403 samples show deeper nitrided layer than those of the SCS6. The fundamental reason is likely due to the difference in the elemental composition (Table 1). The SUS403 and SCS6 XRD patterns do not differ much in silica, manganese, phosphor, sulfur, and chromium elements. The major different is nickel, in which the amount of nickel in SCS6 is almost 20 times of that in SUS403. This nickel element might be the main reason that deters the nitrogen penetration. In addition, the present of nickel could also change the hardness for some cases in stainless steel [4].

Considering the processing time variations in both steels, we found that the longer nitrided processing time is applied, the deeper nitrided layer can be obtained. Both types of samples showed that the 40 hours of nitriding process is the best condition to gain the deepest nitrided layer. In addition, when the samples were tested at less than 100 μm, the hardness value is more than the original condition, vertical dot and dashed line in Figs. 4(a) and (b). This is in a good agreement with the micrograph image of the samples (paneled images in Figs. 1 and 2).

4. Conclusion

Analyses onto the effect of nitriding time using the plasma process on the crystal structure/phase and the hardness of commercially available stainless steel SUS403 and SCS6 has been reported. The results show that the addition of nitrogen has a significant role in controlling the microstructure, phase balance, and hardness profile of the materials. The processing time influences the nitrogen penetration phenomenon, which leads to the change in the thickness of nitrided layer and the composition of formed iron nitride. It is revealed that the processing time of 20 hours is sufficient to form an Fe_4N compound. Longer processing time will create a thicker Fe_4N layer in the materials. The present study also found that the use of SUS403 and SCS6 results in different iron nitride characteristics, i.e., crystal structure/phase and surface hardness profile. At last, we discussed the formation mechanism of iron nitride compound-layer during plasma nitriding process.

Acknowledgements

A.B.D.N acknowledged RISTEK DIKTI for grant-in-aid in Penelitian Terapan Unggulan Perguruan Tinggi Negeri (PTUPT) and Penelitian Unggulan Strategi Nasional (PUSN).

References

1. Saravanan, P.; Sakar, M.; Vinod, V.; Cernik, M.; and Balakumar, S. (2015). Large scale synthesis and formation mechanism of highly magnetic and stable iron nitride (ε-Fe3N) nanoparticles. *RSC Advances*, 5(69), 56045-56048.

2. Zulhijah, R.; Nandiyanto, A.B.D.; Ogi, T.; Iwaki, T.; Nakamura, K.; and Okuyama, K. (2014). Gas phase preparation of spherical core–shell α″-$Fe_{16}N_2/SiO_2$ magnetic nanoparticles. *Nanoscale*, 6(12), 6487-6491.
3. Zhang, H.; Gong, Q.; Ren, S.; Arshid, M.A.; Chu, W.; and Chen, C. (2018). Implication of iron nitride species to enhanced catalytic activity and stability of carbon nanotubes supported Fe catalysts for carbon-free hydrogen via low temperature ammonia decomposition. *Catalysis Science and Technology*, 2018(3), 1-10.
4. Muthupandi, V.; Srinivasan, P.B.; Shankar, V.; Seshadri, S.; and Sundaresan, S. (2005). Effect of nickel and nitrogen addition on the microstructure and mechanical properties of power beam processed duplex stainless steel (UNS 31803) weld metals. *Materials Letters*, 59(18), 2305-2309.
5. Tayal, A.; Gupta, M.; Pandey, N.; Gupta, A.; Horisberger, M.; and Stahn, J. (2015). Effect of Al doping on phase formation and thermal stability of iron nitride thin films. *Journal of Alloys and Compounds*, 650, 647-653.
6. Czerwinski, F. (2012). Heat Treatment-Conventional and Novel Applications. Retrieved on December 2017, from https://www.researchgate.net/profile/Fathollah_Sajedi/publication/231336919_Heat_Treatment-_Conventional_and_Novel_Applications/links/09e4150683d7f0e5d5000000/Heat-Treatment-Conventional-and-Novel-Applications.pdf.
7. Xi, Y.-t.; Liu, D.-x.; and Han, D. (2008). Improvement of corrosion and wear resistances of AISI 420 martensitic stainless steel using plasma nitriding at low temperature. *Surface and Coatings Technology*, 202(12), 2577-2583.
8. Liem, L.; Triawan, F.; and Maeda, H. (2015). Surface characteristics of plasma nitrided 12% chrome steels. *Proceedings of the 6th International Conference on Manufacturing, Machine Design, and Tribology*. Okinawa, Japan, 1-2.
9. Hibi, M.; Triawan, F.; Inaba, K.; Takahashi, K.; Kishimoto, K.; Hayabusa, K.; and Nakamoto, H. (2018). Cavitation damage of epoxy resin subjected to uniaxial tensile loading. *Mechanical Engineering Journal*, 5(1), 17-00151-00117-00151.
10. Kojima, T.; Inaba, K.; Takahashi, K.; Triawan, F.; and Kishimoto, K. (2017). Dynamics of wave propagation across solid–fluid movable interface in fluid–structure interaction. *Journal of Pressure Vessel Technology*, 139(3), 031308.
11. Nurprasetio, I.P.; Budiman, B.A.; and Triawan, F. (2017). Failure investigation of plastic shredding machine's flange coupling based on mechanical analysis. *Indonesian Journal of Science and Technology*, 2(2), 124-133.
12. Hiraoka, Y.; and Ishida, A. (2017). Effect of compound layer thickness composed of γ'-Fe4N on rotated-bending fatigue strength in gas-nitrided JIS-SCM435 steel. *Materials Transactions*, 58(7), 993-999.
13. Jiang, L.; and Gao, L. (2006). Fabrication and characterization of Fe 3 O 4/CNTs and Fe 2 N/CNTs composites. *Journal of Electroceramics*, 17(1), 87-90.
14. Ogi, T.; Nandiyanto, A.B.D.; Kisakibaru, Y.; Iwaki, T.; Nakamura, K.; and Okuyama, K. (2013). Facile synthesis of single-phase spherical α″-$Fe_{16}N_2/Al_2O_3$ core-shell nanoparticles via a gas-phase method. *Journal of Applied Physics*, 113(16), 164301.

15. Park, M.J.; Lee, J.H.; Hembram, K.; Lee, K.-R.; Han, S.S.; Yoon, C.W.; Nam, S.-W.; and Kim, J.Y. (2016). Oxygen reduction electrocatalysts based on coupled iron nitride nanoparticles with nitrogen-doped carbon. *Catalysts*, 6(6), 86.
16. Tatarova, E.; Guerra, V.; Henriques, J.; and Ferreira, C.M. (2007). Nitrogen dissociation in low-pressure microwave plasmas. *Journal of Physics: Conference Series*, 71, 012010.
17. Zulhijah, R.; Nandiyanto, A.B.D.; Ogi, T.; Iwaki, T.; Nakamura, K.; and Okuyama, K. (2015). Effect of oxidation on α″-$Fe_{16}N_2$ phase formation from plasma-synthesized spherical core–shell α-Fe/Al_2O_3 nanoparticles. *Journal of Magnetism and Magnetic Materials*, 381, 89-98.
18. Zulhijah, R.; Yoshimi, K.; Nandiyanto, A.B.D.; Ogi, T.; Iwaki, T.; Nakamura, K.; and Okuyama, K. (2014). α″-$Fe_{16}N_2$ phase formation of plasma-synthesized core–shell type α-Fe nanoparticles under various conditions. *Advanced Powder Technology*, 25(2), 582-590.
19. Corengia, P.; Ybarra, G.; Moina, C.; Cabo, A.; and Broitman, E. (2004). Microstructure and corrosion behaviour of DC-pulsed plasma nitrided AISI 410 martensitic stainless steel. *Surface and Coatings Technology*, 187(1), 63-69.
20. Pinedo, C.E.; and Monteiro, W.A. (2004). On the kinetics of plasma nitriding a martensitic stainless steel type AISI 420. *Surface and Coatings Technology*, 179(2-3), 119-123.
21. Sun, Y.; Bell, T.; and Wood, G. (1994). Wear behaviour of plasma-nitrided martensitic stainless steel. *Wear*, 178(1-2), 131-138.
22. Al-Aqeeli, N. (2012). Wear and Mechanical Properties' Evaluation of Duplex-Treated Ti-6Al-4V Alloy Using Nanoindentation. *Arabian Journal for Science and Engineering*, 37(3), 735-748.
23. Tosun, G. (2014). Coating of AISI 1010 steel by Ni–WC using plasma transferred arc process. *Arabian Journal for Science and Engineering*, 39(4), 3271-3277.